



Supplement of

The Scotland–Canada overturning array (SCOTIA): twenty years of meridional overturning in the subpolar North Atlantic

Alan D. Fox et al.

Correspondence to: Neil J. Fraser (neil.fraser@sams.ac.uk)

The copyright of individual parts of the supplement might differ from the article licence.

Supplementary Information

S.1 Construction of the SCOTIA Θ - S climatology

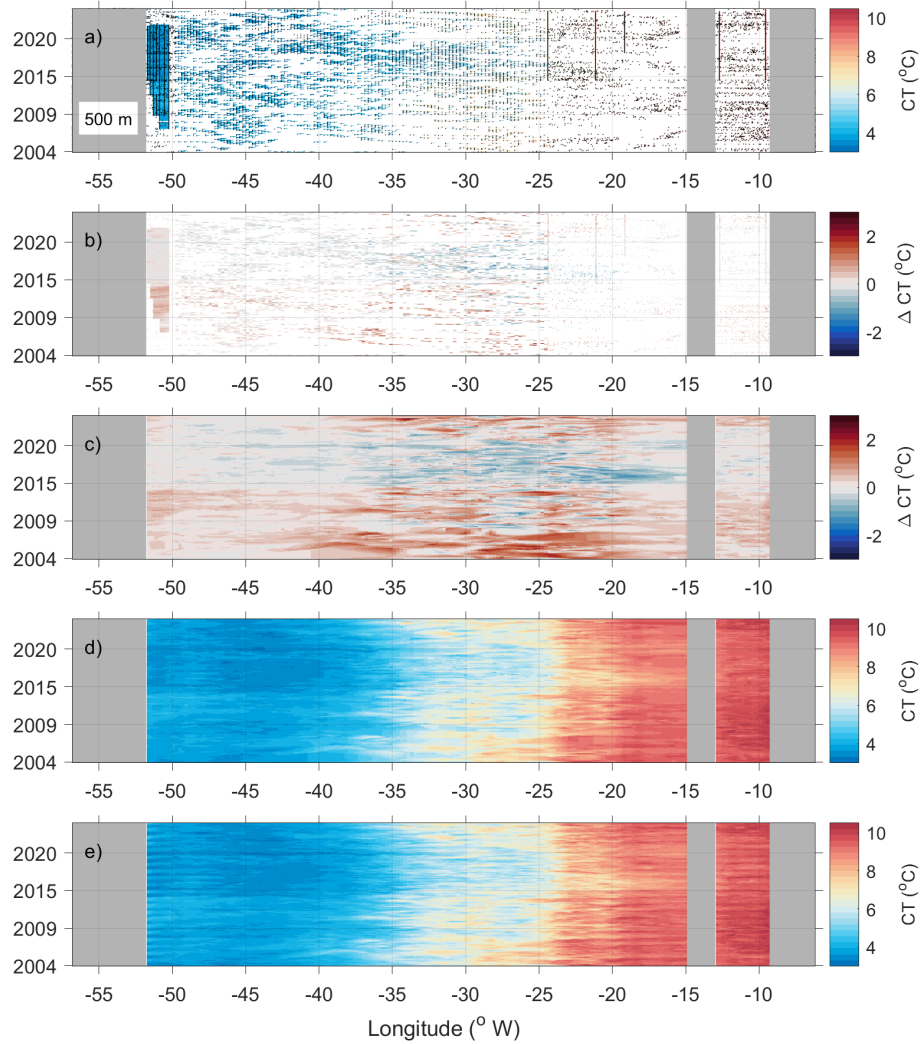


Figure S1: Construction of time-varying gridded Θ - S fields. This example shows a slice of the 3D Conservative Temperature (Θ /CT) field at 500 m depth. Note smaller grid cells west of 50° W and east of 25° W. Grey regions show where the depth level intersects with bathymetry. a) Gridded observations from scattered CTD and Argo profiles, and fixed moorings. Individual observations shown by black points, b) gridded observations: anomaly computed by subtracting local mean and seasonal cycle (derived from monthly mean seasonal climatology), c) 3D linear interpolation between gridded observed anomalies, d) anomaly + local mean, showing de-seasoned variability, e) anomaly + local mean + local seasonal cycle, showing total variability.

S.2 Compensation velocities

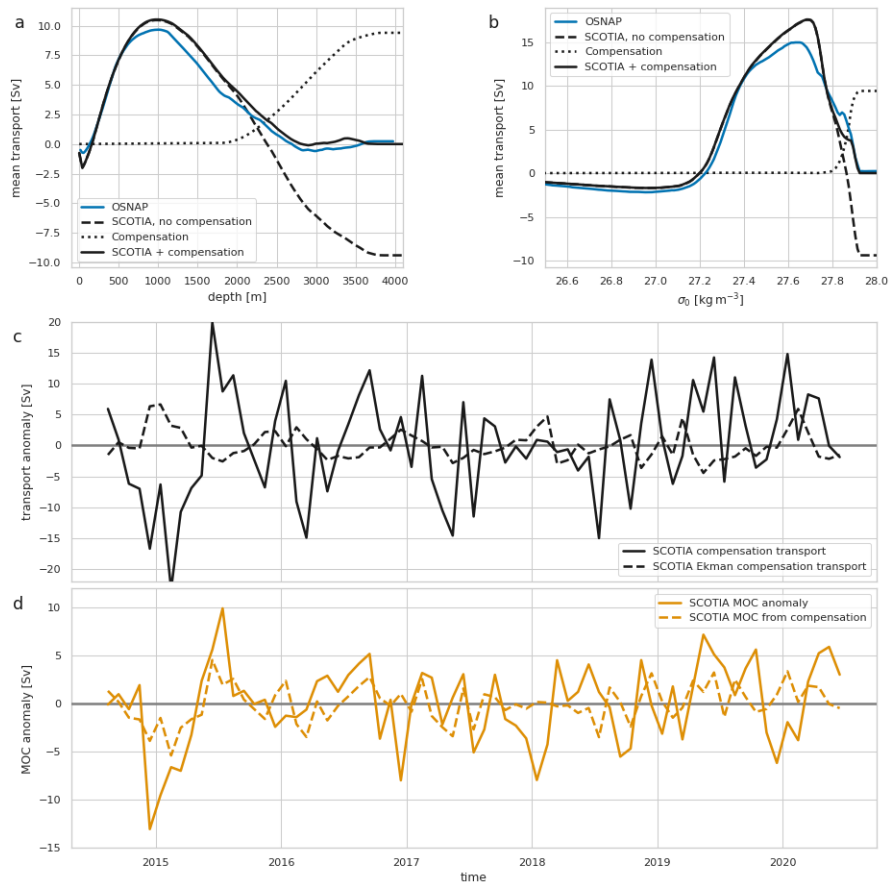


Figure S2: SCOTIA compensation transport and its effects on the estimate of overturning. Panels (a) and (b) show the mean (over the OSNAP period) overturning streamfunctions in depth and density space respectively. In each case the dashed black line is the SCOTIA mean streamfunction with no compensation applied, the dotted black line is the contribution to the streamfunction from compensation, and the solid black line is the resulting SCOTIA mean overturning streamfunction including compensation. The OSNAP mean streamfunction is shown in blue for comparison. Panel (c) shows the time-varying part of the compensation transport, again covering the OSNAP period. The solid black line is the total compensation anomaly, the dotted black line the part of this compensation required to balance surface Ekman transports. In panel (d), the solid amber line is the MOC anomaly, and the dotted amber line is the part of the MOC anomaly directly contributed by the compensation transport.

S.3 Modelling

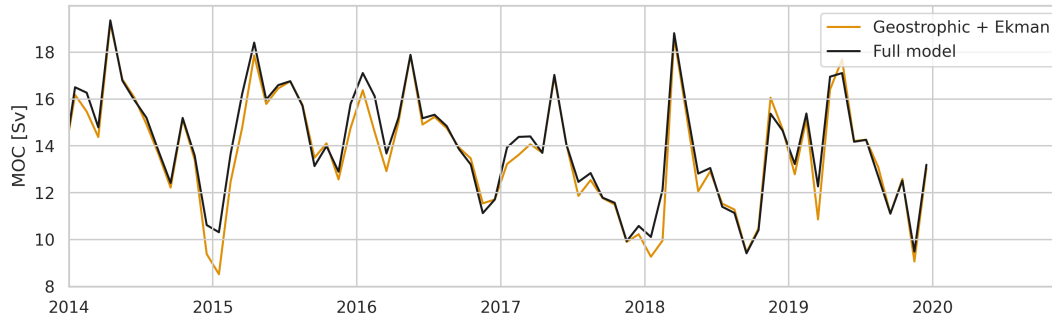


Figure S3: time series of **modelled** overturning on across SCOTIA comparing the full model MOC with that calculated using geostrophy, from model Θ -S, referenced to model sea surface height, plus surface Ekman transport. Geostrophic currents are seen to dominate the overturning.

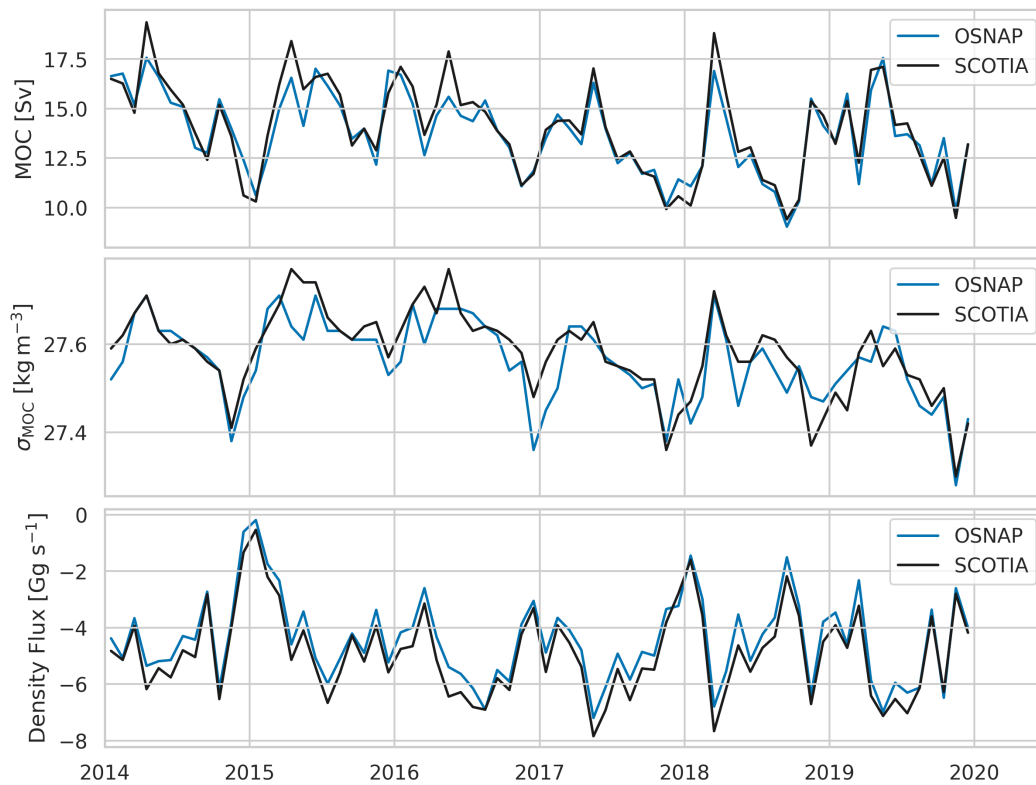


Figure S4: Comparison of **modelled** MOC (top panel), σ_{MOC} (middle panel) and density flux (lower panels) across OSNAP (blue lines) and SCOTIA (black lines) sections.

S.4 SCOTIA calculations

In constructing the SCOTIA observational time series of overturning and transports we encountered various options for calculation of temperature, salinity and velocities. Here we present a brief comparison of some those options and their performance.

We have primarily assessed success through comparison of SCOTIA results with OSNAP data for the period 2014 to 2020, the results of these comparisons are seen in Table S1. The final selected calculation, which we just refer to as SCOTIA is to use the gridded Θ - S fields across the whole section with velocities calculated using geostrophy relative to satellite ADT

at the surface, but replacing the shelf Θ , S and v data with GLORYS output.

	OSNAP	SCOTIA	No moorings	Uniform comp.	No GLORYS	Mooring velocities
mean MOC [Sv]	16.51	18.29	18.21	19.35	16.39	17.44
s.d. MOC [Sv]	3.30	3.83	4.36	3.94	3.82	3.90
correl. MOC		0.66	0.61	0.64	0.66	0.60
mean σ_{MOC} [kg m^{-3}]	27.62	27.67	27.67	27.70	27.67	27.66
s.d. σ_{MOC} [kg m^{-3}]	0.06	0.06	0.05	0.05	0.06	0.06
correl. σ_{MOC}		0.32	0.22	0.27	0.32	0.31
mean \mathcal{D} [Gg]	-5.47	-6.00	-5.94	-6.35	-4.56	-5.54
s.d. \mathcal{D} [Gg]	1.68	1.97	2.18	1.938	1.96	2.15
correl. \mathcal{D}		0.63	0.55	0.63	0.63	0.66
mean \mathcal{H} [PW]	0.506	0.532	0.538	0.600	0.535	0.532
s.d. \mathcal{H} [PW]	0.064	0.069	0.082	0.068	0.068	0.079
correl. \mathcal{H}		0.35	0.32	0.33	0.34	0.40
mean \mathcal{F} [Sv]	-0.356	-0.370	-0.377	-0.428	-0.426	-0.384
s.d. \mathcal{F} [Sv]	0.054	0.060	0.066	0.059	0.059	0.059
correl. \mathcal{F}		0.49	0.46	0.52	0.52	0.48

Table S1: Comparison between SCOTIA and OSNAP overturning metrics from the section calculations incorporating different data. Comparisons are presented for MOC, the density of maximum overturning (σ_{MOC}), density flux (\mathcal{D}), heat flux (\mathcal{H}), and freshwater flux (\mathcal{F}). In each case the mean, standard deviation, and (for SCOTIA) correlation with OSNAP are presented. The columns refer to SCOTIA calculations incorporating different data: SCOTIA – the final SCOTIA dataset using Θ , S , ADT, geostrophy, separate compensation for mean and anomalies, and GLORYS model data on the shelves; No moorings – omits the OSNAP mooring TS data from the anomaly calculations; Uniform compensation – uses a spatially uniform compensation velocity rather than separate compensation for mean and anomaly; No GLORYS – omits the GLORYS model data on the shelves; Mooring velocities – replaces the geostrophic calculation with directly observed velocities at the western boundary and Rockall Trough. In each line the ‘best’ results are highlighted in blue, and the worst in red. Here ‘best’ means closest to OSNAP for mean and standard deviation and highest correlation, except for mean MOC where we additionally highlight the best value *higher* than the OSNAP estimate as modelling shows overturning at SCOTIA to be slightly above that at OSNAP.

The ‘No moorings’ calculation excluded Θ - S data from the OSNAP moorings in the anomaly calculations. This comparison is useful as prior to 2014 these mooring data are not available. It is reassuring to note that the exclusion of these data does not change the mean

values significantly, does not introduce trends in the observed time series and appears to retain the longer term signals. Significant skill in reproducing OSNAP results is still demonstrated by these estimates, though correlations with OSNAP are reduced by exclusion of this mooring data.

The ‘uniform compensation’ option explored the effects of replacing the separate compensation of mean and anomalies in the transport balance with a more conventional uniform compensation velocity. Using this method MOC and density flux are estimated, though their variability and correlation are less affected. This is expected as the difference between compensation schemes is in how the mean transport imbalance is treated. Most notably, uniform compensation leads to an unrealistic overestimation of the density of maximum overturning, σ_{MOC} . For these reasons we focus on cases with the separated mean and anomaly compensation in the following cases.

The GLORYS model output was tested on the shelves because SC_0 appeared to be overestimating the southward flow on the Labrador shelf when compared to OSNAP (which uses GLORYS). This overestimate of southward-flowing surface water volumes compared to OSNAP is responsible for the slightly low estimates of mean overturning and density flux in SC_0. Replacing the shelf Θ , S , v data (where we have relatively few observations) with GLORYS output (SC_GL) corrects this underestimate, giving estimates of mean overturning and density flux slightly higher than OSNAP, as predicted by the modelling, without making any other significant changes to the variability or correlations. We choose to use GLORYS shelf data in the results presented in the main body of this paper purely because it produces results for SCOTIA which are closer to those from OSNAP, although we acknowledge that this may not be a good guide to which method is ‘better’.

Finally, we replace SCOTIA Θ , S and v on the western boundary and in the Rockall Trough

with gridded Θ , S and v from the OSNAP moorings. These are regions of strong, complex flows over steep topography where the assumption of geostrophy is likely to be less reliable. The incorporation of this additional mooring data offers little advantage over the base SCOTIA calculation while potentially introducing a discontinuity in the SCOTIA dataset at the start of the OSNAP period.



Figure S5: As Fig. 4, but with Θ - S anomalies from moorings omitted from the calculation. These data do still inform the monthly seasonal climatology.

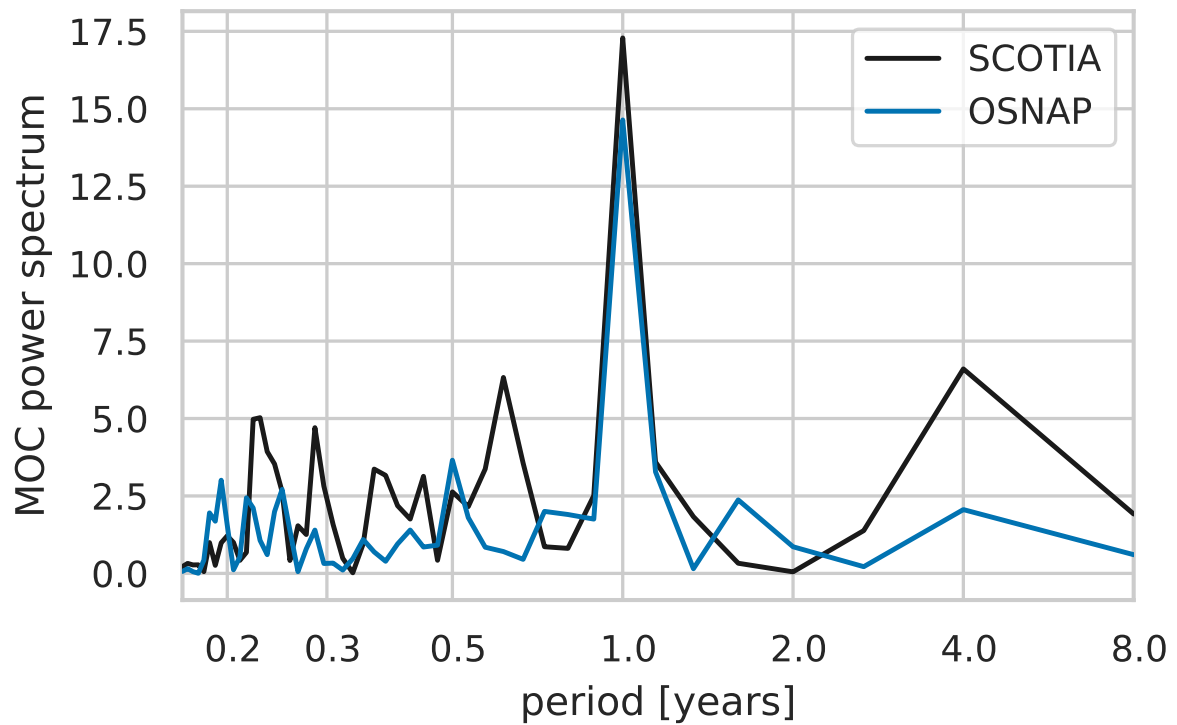


Figure S6: Power spectra for the SCOTIA and OSNAP MOC time series for the period 2014 to 2022.

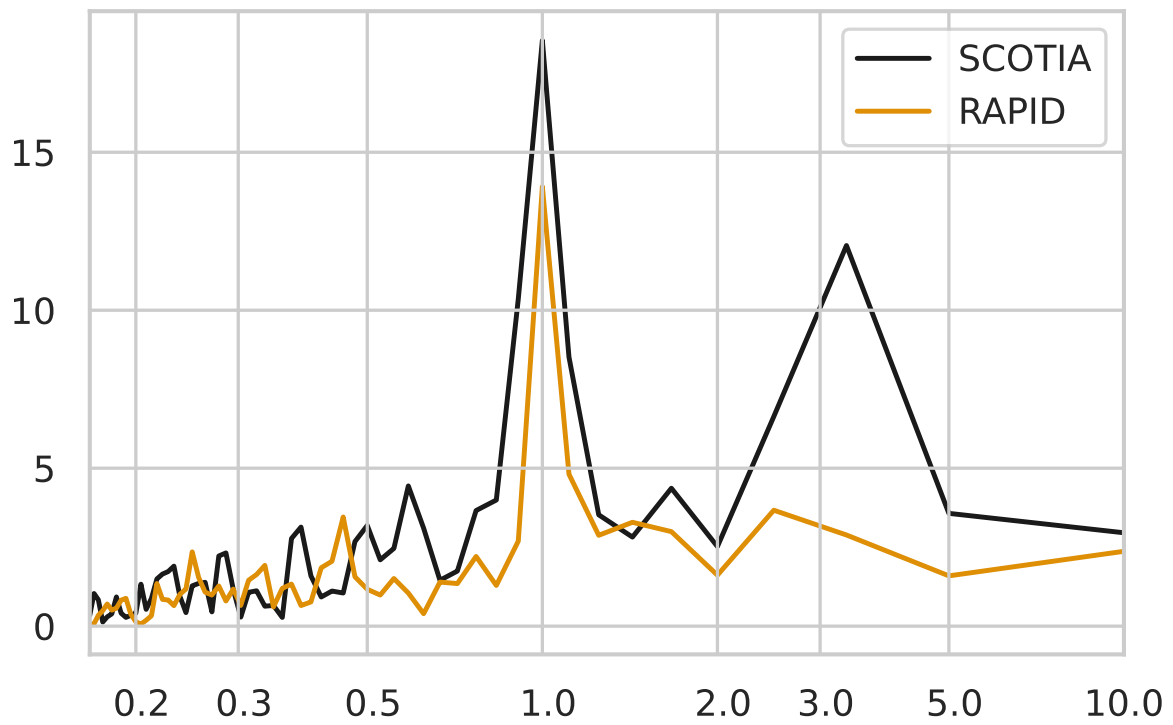


Figure S7: Power spectra for the SCOTIA and RAPID MOC time series for the period 2004 to 2024.

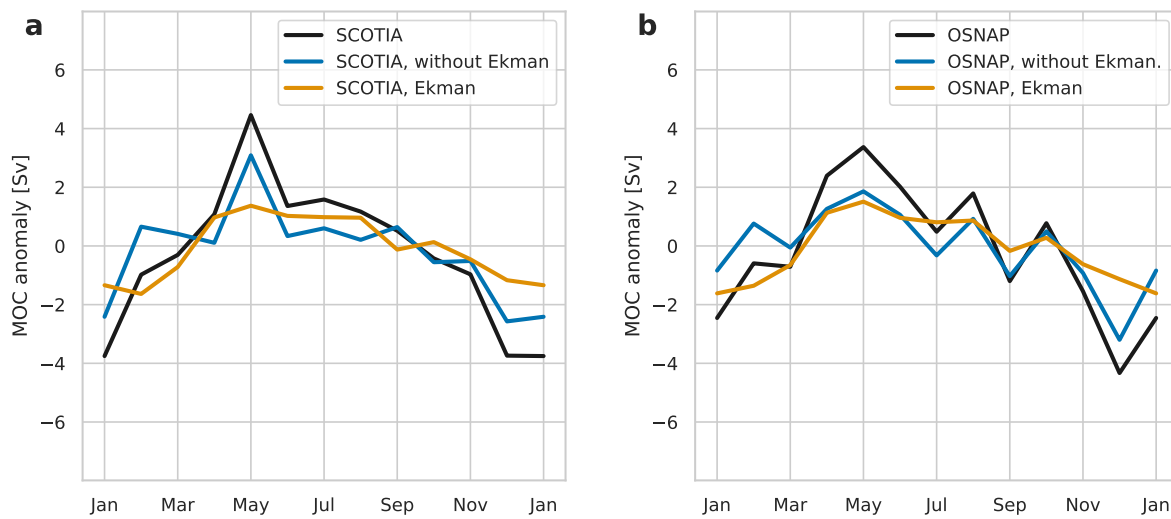


Figure S8: MOC seasonal cycle for (a) SCOTIA and (b) OSNAP. The surface Ekman contribution is diagnosed as the difference between the full overturning and that obtained after removing surface Ekman transports (with compensation). Ekman transport is applied in the surface grid cell at OSNAP; distributing it over the upper 50 m yields negligible differences. The Ekman contribution is nearly identical between the two sections, reflecting the close proximity of the two lines relative to the horizontal scale of weather patterns.

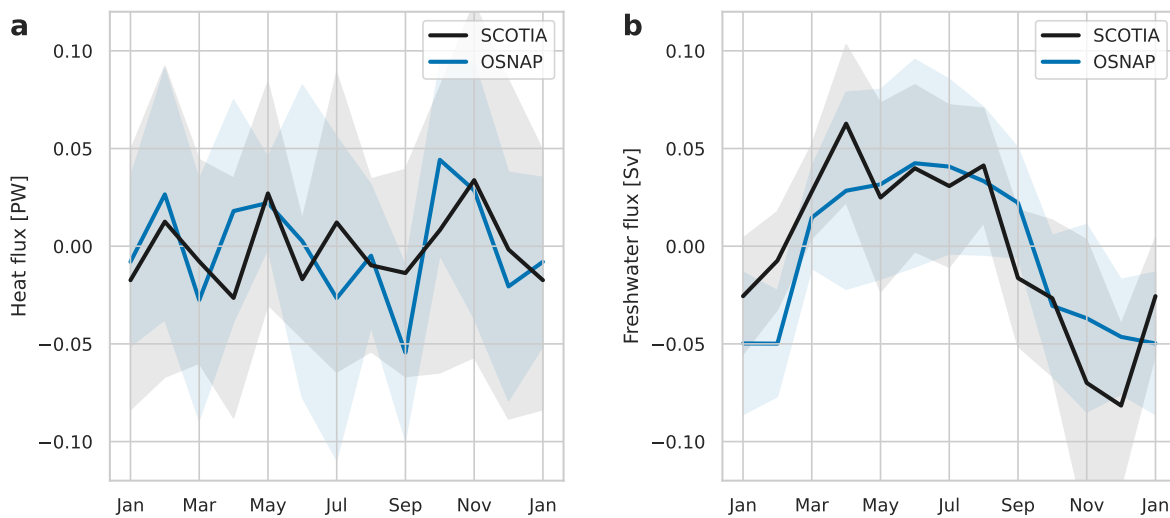


Figure S9: Seasonal cycles of (a) heat flux and (b) freshwater flux across the SCOTIA and OSNAP sections. Heat flux exhibits no clear or coherent annual cycle in either section. In contrast, freshwater flux shows a broadly consistent seasonal cycle between the two, with some divergence during winter months. Shaded regions indicate ± 1 standard deviation of monthly variability.